Supporting Information

An endogenous enzyme-triggered multivariate-gated DNA nanosystem for high-fidelity tumour cell recognition

Yuzheng Zhou, Die Hu, Xiang Li, Yang Xu, Hong Zhou, Peng He**

[†]Key Laboratory of Optic-electric Sensing and Analytical Chemistry for Life Science, MOE, Shandong Key Laboratory of Analytical Chemistry for Life Science and Intelligent Detection, College of Chemistry and Molecular Engineering, Qingdao University of Science and Technology, Qingdao 266042, P. R. China.

*Corresponding author: hepeng@qust.edu.cn (Peng He); zhouhong@qust.edu.cn (Hong Zhou)

TABLE OF CONTENTS

Experimental section

Materials

1,2-Dioleoyl-sn-glycero-3-phosphate choline, cholesterol and 1,2-distearoyl-sn-glycero-3-phosphoethanolamine-N-[maleimide (polyethylene glycol) 2000], magnesium chloride, tris(hydroxymethyl)aminomethane (Tris), and hydrochloric acid were purchased from Aladdin Co. (Shanghai); 50× TAE and acrylamide were purchased from Sangyo Bio Co. Structure-specific nuclease (FEN1), T7 nucleic acid exonuclease (T7 EXO), and nucleic acid exonuclease 1 (EXO I) were purchased from New England Biotech (USA); human purine-free/pyrimidine-free nucleic acid endonuclease 1 (APE1) was purchased from New England BioLabs Co. Ltd. (Beijing, China); ethidium bromide was purchased from Shanghai Sangong Biotechnology Co. Ltd. (Wuhan, China); RPMI-1640, DMEM medium, phosphate buffer solution (PBS) were purchased from KeyGen Biotechnology (Nanjing, China); trypsin was purchased from China Medical Co Ltd; CCK-8 kits were purchased from Sangon Biotech Co Ltd. Ltd (Shanghai, China); all other reagents were of analytical grade.

Apparatus

The zeta potential and dynamic light scattering particle size analysis system used in this experiment was provided by PMX, Germany; transmission electron microscope (model: JEM-2000EX) was purchased from Hitachi, Japan; carbon dioxide constant temperature cell incubator was from Blue Leopard Experimental Instruments (Shanghai); fluorescence detection was carried out with the F-7000 Fluorescence Spectrophotometer (Hitachi, Japan); the cell

confocal The fluorescence images were obtained by confocal microscope (Leica, Germany); the kinetic particle size analyser was from PMX, Germany; the atomic force microscope was from Vecco, USA; the enzyme marker for cell viability was from Bio-Tek, USA; the electrophoresis instrument and electrophoresis tank were from Beijing Junyi Oriental Co.

Native polyacrylamide gel electrophoresis (PAGE)

This study employed 12% polyacrylamide gel electrophoresis (PAGE) to analyze DNA samples. Prior to the experiment, the glass plates and comb were thoroughly rinsed with deionized water, air-dried, and then assembled into the electrophoresis apparatus according to standard operating procedures. The gel preparation process was as follows: Accurately measure 5.256 mL of ultrapure water, 2.5 mL of acrylamide monomer solution, 160 μL of 50× TAE buffer, 4 μL of TEMED catalyst, and 80 μL of 50% ammonium persulfate (APS) solution. Thoroughly mix the solution and pour it into the interlayer of the glass plates. The gel polymerizes at room temperature for 2 hours and is ready for use once fully cured. For sample preparation, mix 10 μL of DNA sample with 2 μL of 6× loading buffer in the specified ratio. Electrophoresis conditions are set as follows: initial voltage of 180 V for 3 minutes, followed by adjustment to 135 V for 1.2 hours. After electrophoresis, the gel is incubated in ethidium bromide staining solution for 20 minutes. Subsequently, image acquisition and analysis are performed under UV light using a gel imaging system.

Atomic Force Microscopy Imaging

The morphology of DNA products (10 μL, 1 μM) in the presence of APE1 activation were

characterized by AFM. The samples were deposited onto a fresh mica surface, and then washed with deionized water for removing buffer and dried them. Finally, the samples were characterized and imaged by a Multi-mode V8 AFM (Bruker) system.

Preparation of Liposomes

In this study, liposomes were prepared by thin film hydration.[1, 2] Specifically, 1,2-dioleoyl-sn-glycero-3-phosphocholine (DOPC, 0.0033 g), cholesterol (0.0016 g), and 1,2-distearoyl-sn-glycero-3-phosphoethanolamine-N-[maleimide (polyethyleneglycol) 2000] (DSPE-PEG-Mal, 0.0014 g) were dissolved in 10.0 mL chloroform , stirring thoroughly until complete dissolution. Subsequently, the mixed solution was transferred to a rotary evaporation flask, maintaining the water bath temperature at 45 °C, and rotary evaporation was achieved in the rotary evaporation flask under reduced pressure, and ultimately the formation of a homogeneous lipid film could be observed on the wall of the flask, and ultrapure water was subsequently added to the flask and sonicated using an ultrasound apparatus, and a homogeneous liposome suspension was obtained after five minutes. Finally, the initially prepared liposome suspension was repeatedly extruded through a polycarbonate membrane in a liposome extruder for 21 times to obtain a liposome dispersion system with uniform particle size. The resulting liposome suspension was stored at 4 °C away from light and used within 24 h to ensure the reliability of the experimental results.

Cell Cytotoxicity Assays

The biocompatibility of the cells was evaluated by using a Cell Counting Kit-8 (CCK-8) assay. MCF-7 and HEK293T cells (1 × 104 cells/well) were seeded respectively in 96-well plates and

cultured at 37 °C in 5 % CO2 for 24 h. When the cells got a suitable density, the cells were incubated with different concentrations of hMNS (0, 20, 40, 60, 80, 100, 120 μg mL-1) for 24 h at 37 °C. Afterward, the cells were washed with PBS three times and mixed with the CCK-8 solution to record the optical density (OD) at 450 nm for measuring the cell viability. The cell viability was calculated using the following equation: Cell Viability = (ODTreated – ODBlank)/(ODControl – ODBlank).

Cell culture

This study employed high-glucose DMEM complete medium (containing 10% FBS, 100 U/mL penicillin and 100 μg/mL streptomycin) for culturing MCF-7 and HEK-293 cell lines. Cell culture conditions were maintained at 37°C with 5% CO_2 saturation humidity. During the experiment, cell growth status must be monitored regularly, with medium changes performed every 1-2 days. When cell confluence reaches 80-90%, cells should be washed three times with sterile PBS buffer, followed by digestion with trypsin for passaging, cryopreservation, or other experimental procedures. All steps must be conducted within a sterile bench to ensure a clean experimental environment. The incubator requires regular cleaning and disinfection. Prior to cell handling, the cell culture chamber must undergo ultraviolet sterilisation and be maintained in a tidy state. For fluorescence imaging experiments, cells are seeded into 35 mm glass culture dishes and incubated overnight in the incubator. Subsequently, cells are washed with PBS and treated with probes at varying concentrations, followed by incubation at 37°C for a specified duration.

Supplementary Figures and Tables

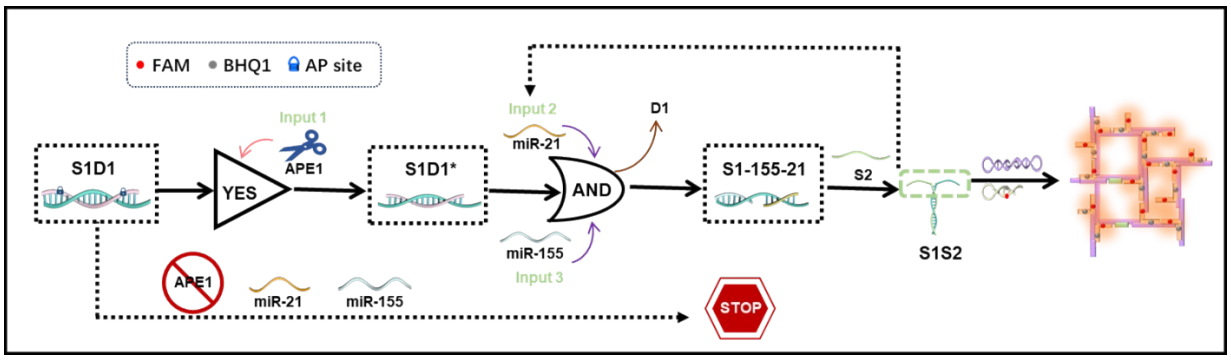

Scheme S1. Detection principle of the "YES-AND"logic detection system.

Our enzyme-triggered ternary "YES-AND" DNA logic gate system comprises two modules: an operational module and an amplification module. As shown in Scheme 1, the operational module comprises the double-chain complexes S1-D1 and S2-D3. By introducing an adduct site (AP) at the 5' end and the eighth nucleotide at the 3' end of the D1 strand, the engineered D1 strand is then combined with the S1 strand to form the S1D1 double-stranded complex. Concurrently, the computational module incorporates an EDC cyclic assembly step, which serves not only as part of the computational unit but also as the promoter for the amplification unit. Within the amplification unit, DHR comprises DNA H1-1, DNA H1-2, and DNA H2. DNA H2 is modified with a fluorophore (FAM) and a quencher (BHQ1), generating low background signal via Förster resonance energy transfer (FRET). Complementary segments on the H1-1 and H1-2 strands can form hairpin dimers through hybridisation. In the presence of APE1, the AP site on D1 is selectively cleaved by APE1, generating a nucleotide gap at both the 5' and 3' ends of D1. Consequently, a 7-nucleotide single-stranded fragment separates from S1-D1, exposing the binding sites on S1: the miR-21 binding site at the 3' end and the miR-155 binding site at the 5' end. In the presence of target I2 (miR-21) or I3 (miR-155), these cleaved promoters remain unchanged with the input miR-155 or miR-21, preventing D1 replacement. Consequently, S1D1 remains stable, leading to erroneous output. Conversely, in the presence of both input I2 and I3, D1 can be effectively displaced, forming a novel ternary complex S1-miR-21-miR-155. This simultaneously exposes the S2 recognition site at the midpoint of S1, allowing fuel DNA S2 to bind. A second consecutive displacement reaction generates the double-stranded complex S1-S2, simultaneously releasing miR-21 and miR-155. The released

miRNAs trigger another TSDR, cyclically inducing the EDC assembly process to generate abundant S1-S2 double-stranded complexes. The cleaved trigger fragments miR-21 and miR-155 generate a T-sequence near the S1-S2 complex, thereby continuously opening the H1 dimer. In the absence of T, the H1 dimer and H2 coexist stably. Treatment of a mixture of H1 dimer and H2 with the double-stranded complex (S1-S2) opens the H1 dimer via a DNA strand displacement reaction. Subsequently, the active H1 dimer opens and activates H2 via the same mechanism. H2 then sequentially opens another H1 dimer. Tandem T sequences can specifically mediate subsequent alternating hybridisation between H1 dimers and H2, forming an extensive DHR dsDNA three-dimensional network. Compared to the linear products of conventional HCR, the EDC-DHR cascade amplification strategy in this system enables specific initiation of amplification reactions in living cells upon APE1 triggering. This generates network structures and significantly amplified fluorescent signals, thereby achieving sensitive target detection. Consequently, the enzyme-activated amplification process of DNA machines enables infinite exponential signal amplification in a simple, isothermal manner. Furthermore, the reliability of our YES-AND logic gate offers tremendous promise for the comprehensive analysis of diverse miRNA patterns across various cancer cells.

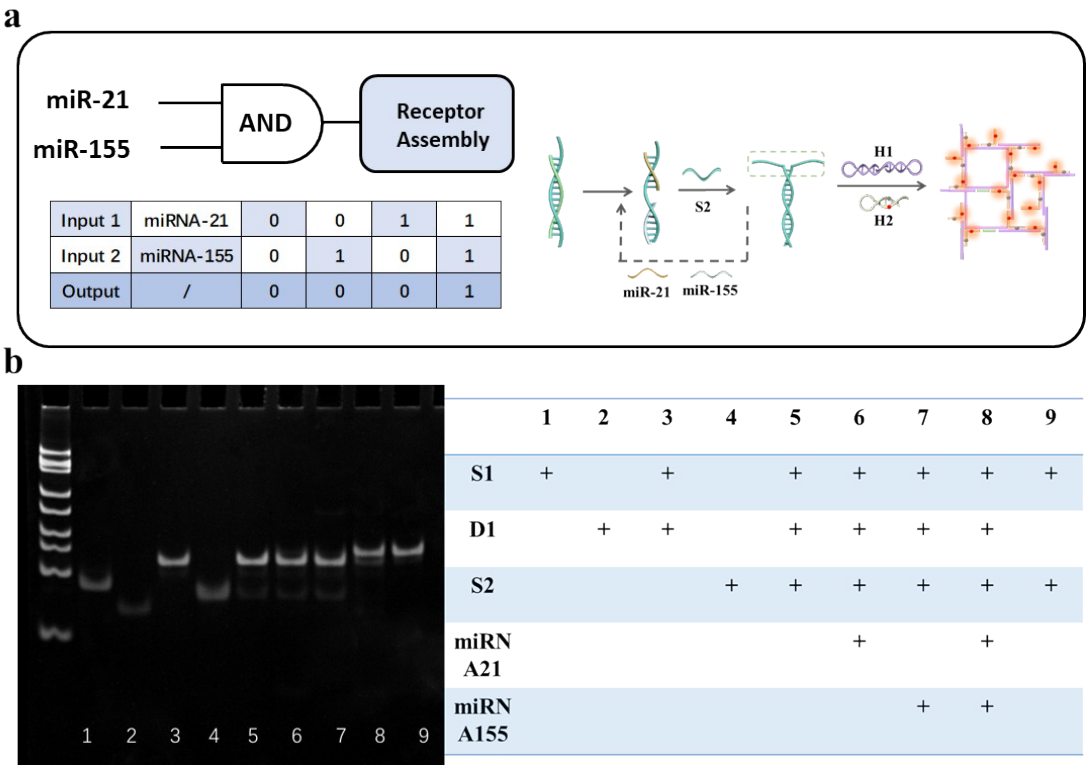

Figure S1. (a) Detection Principle and (b) PAGE Feasibility Analysis of the AND Logic Detection System.

As shown in Figure S1b, the results of polyacrylamide gel electrophoresis (PAGE) experiments confirmed the feasibility of the AND logic gate, and our designed AND logic circuit specifically triggered only when both miRNA-21 and miRNA-155 were present simultaneously.

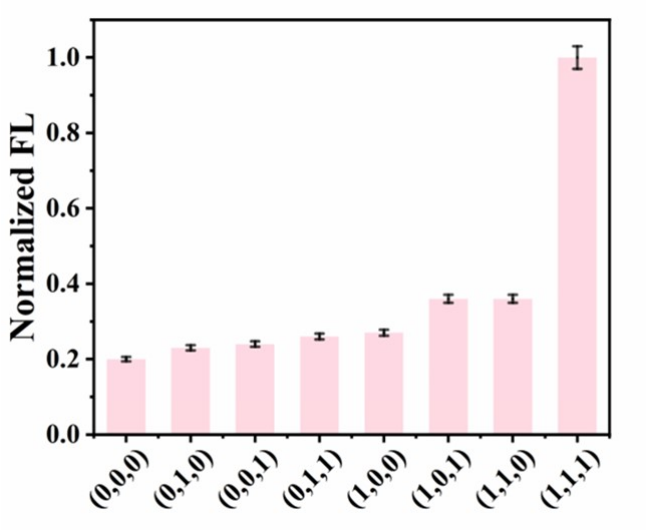

Figure S2. Relative fluorescence intensity of DNA probes under different combinations of APE1 and miR-21, miR-155.

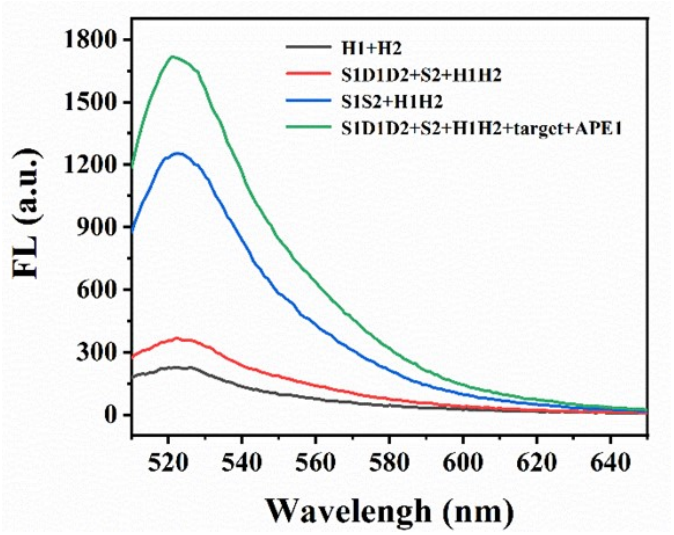

Figure S3. Fluorescence spectral analysis of DNA probes lacking different components.

a

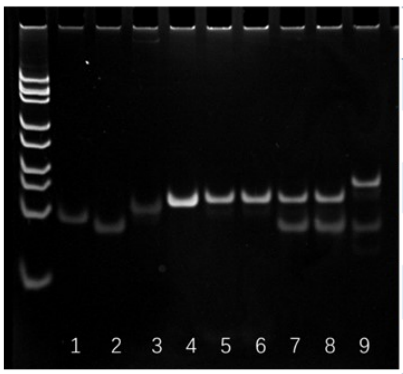

	1	2	3	4	5	6	7	8	9
S1	+			+	+	+	+	+	+
D1			+	+	+	+	+	+	+
S2		+					+	+	+
APE1					+	+	+	+	+
miRNA21					+		+		+
miRNA155						+		+	+

b

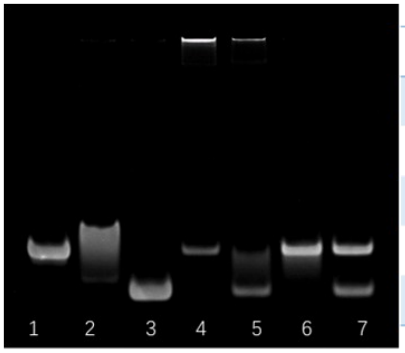

	1	2	3	4	5	6	7
S1	+			+		+	+
S2	+			+		+	+
H1-1		+		+	+	+	
H1-2		+		+	+	+	
H2			+	+	+		+

Figure S4. Verification of (a) EDC feasibility and (b) DHR feasibility via PAGE analysis.

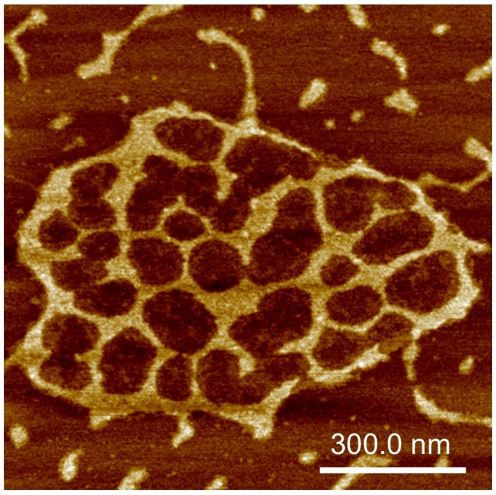

Figure S5. AFM image of the DNA Network.

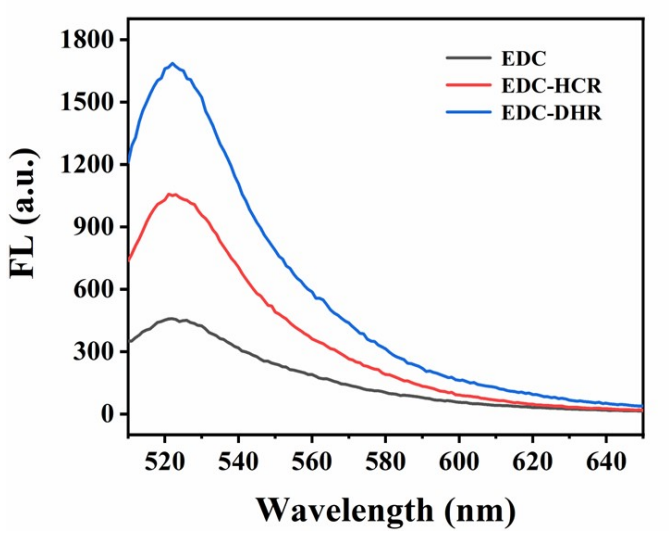

Figure S6. Fluorescence spectra corresponding to the EDC system, EDC-HCR system, and EDC-DHR system measured under identical conditions and probe concentrations..

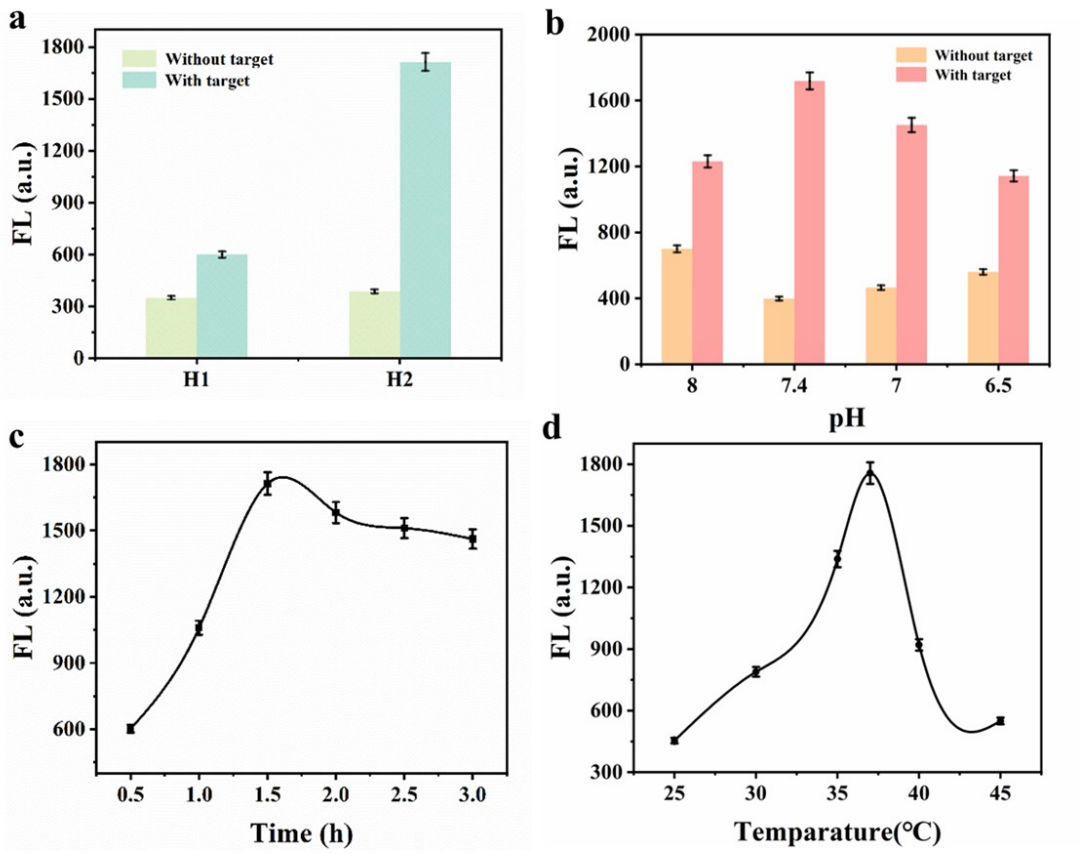

Figure S7. (A) Comparison of fluorescence intensity when fluorescent groups are modified on H1 and H2 respectively. (B) Variation in maximum fluorescence intensity of the logic platform at different pH values. (C) Optimisation of reaction time. (D) Optimisation of reaction temperature. Data error bars represent mean ± SD (n=3).

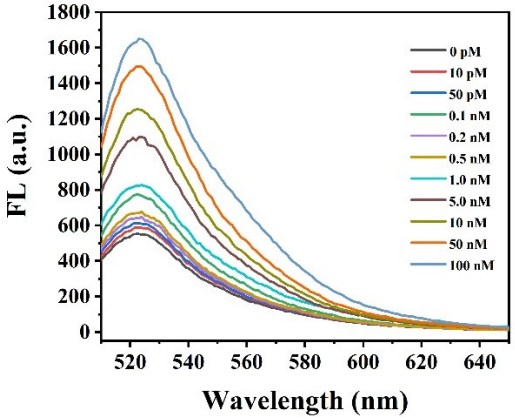

Figure S8. Fluorescence intensity response curves of different concentrations of miRNA-21 when adding equal amounts of APE1 (10 U/ml) and miRNA-155 (10^{-7} M).

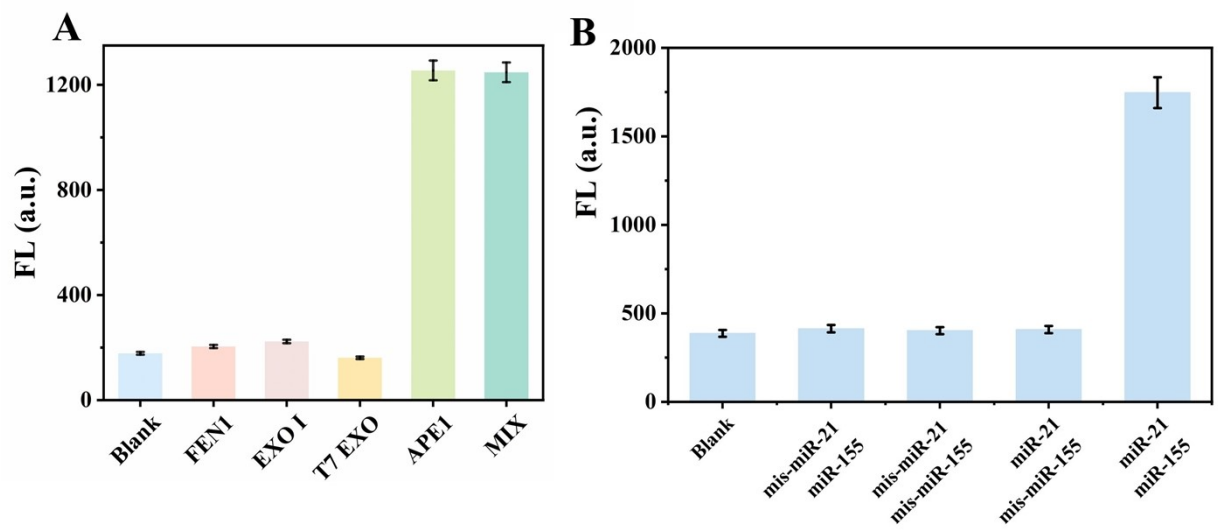

Figure S9. (A) Selectivity of APE1 at the addition of the same amount of miR-21 and miR-155 (1×10^{-7} M) (both at a concentration of 10 U/mL). (B) Relative fluorescence intensity of the nanoprobe upon addition of mis-miR-21 (1.0×10^{-7} M) and mis-miR-155 (1.0×10^{-7} M).

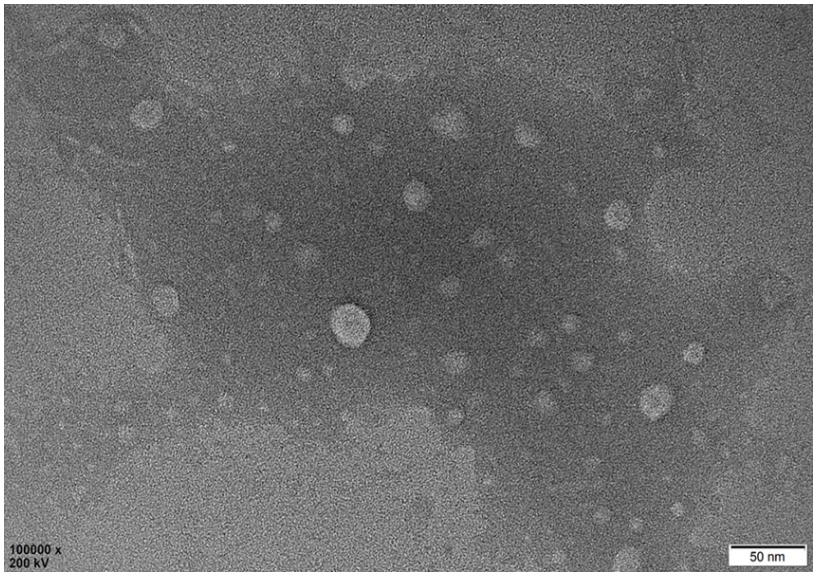

Figure S10. TEM images of LNPs.

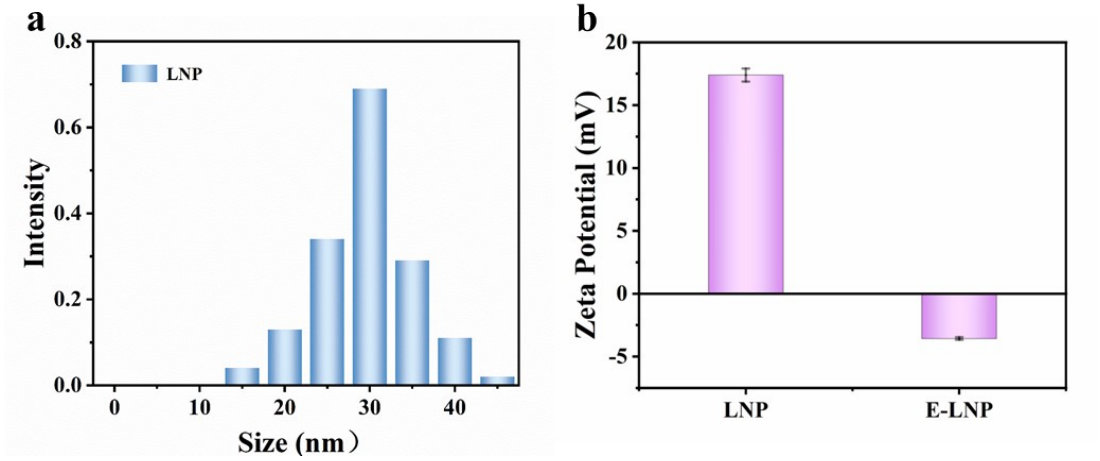

Figure S11. (A) Particle size distribution of LNP. (B) Zeta potential characterisation of LNP and E-LNP loaded with DNA probes. Data error bars denote mean ± SD (n=3).

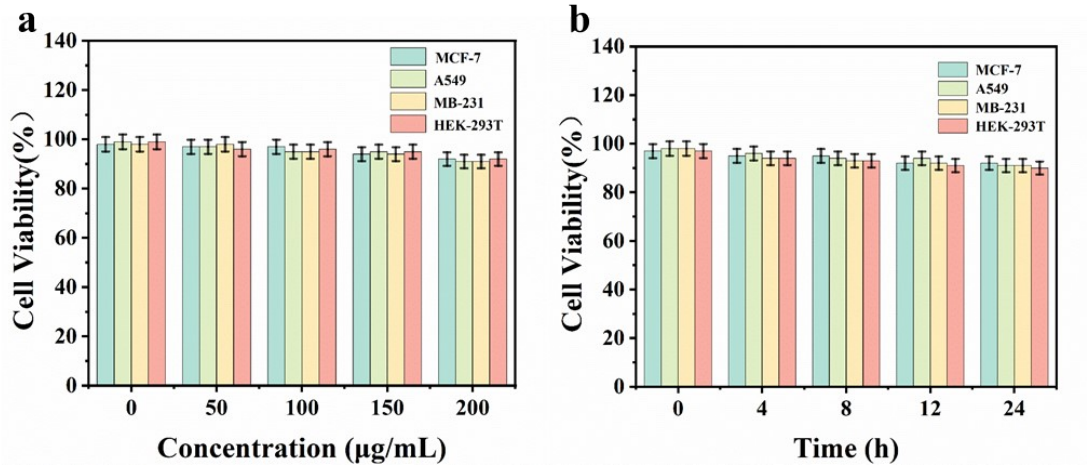

Figure S12. Cytotoxicity analysis of MCF-7, A549, MDA-MB-231, and HEK-293T cell lines treated with E-LPN-based YES-AND logic DNA nanoprobes. (A) Cells were incubated with varying concentrations of nanoprobes for 24 hours. (B) Cells were treated with 100 μg/mL nanoprobes for different incubation durations. All data are presented as mean ± SD (n=3).

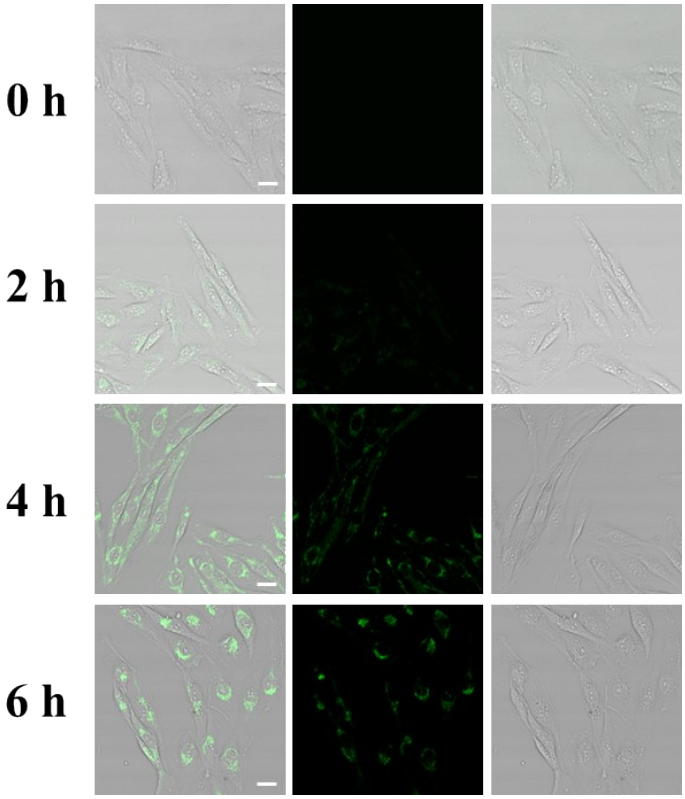

Figure S13. Confocal laser scanning microscopy images of MDA-MB-231 cells incubated with nanoprobes at different time points. Scale bar: 25μm.

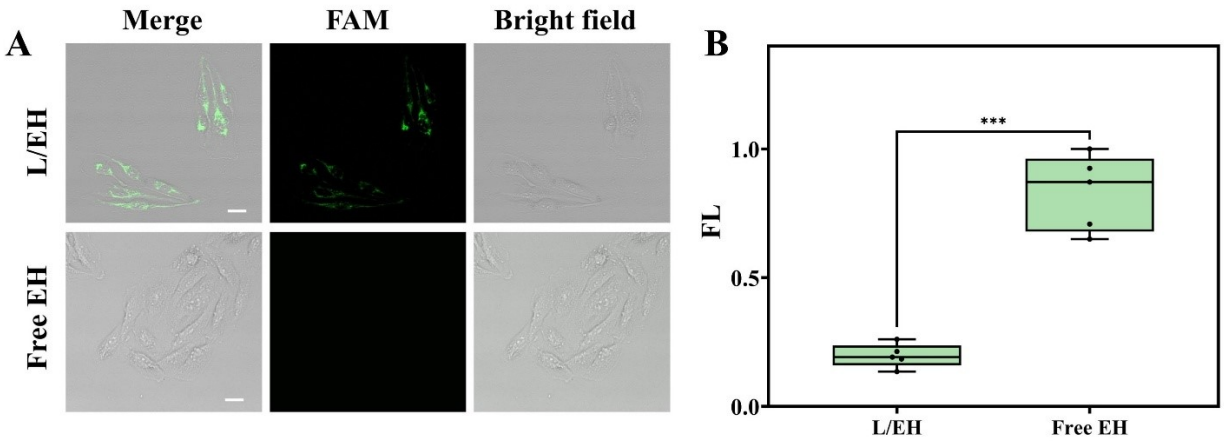

Figure S14. (A) Confocal laser scanning microscopy (CLSM) images of MDA-MB-231 cells incubated with L/EH nanosystem or free EH. From left to right: merged images, FAM fluorescence channel, bright-field channel. Scale bar: 25 μm. (B) Quantification of FAM fluorescence intensity in (A), with data as mean ± SD (n=5, ***$p < 0.001$).

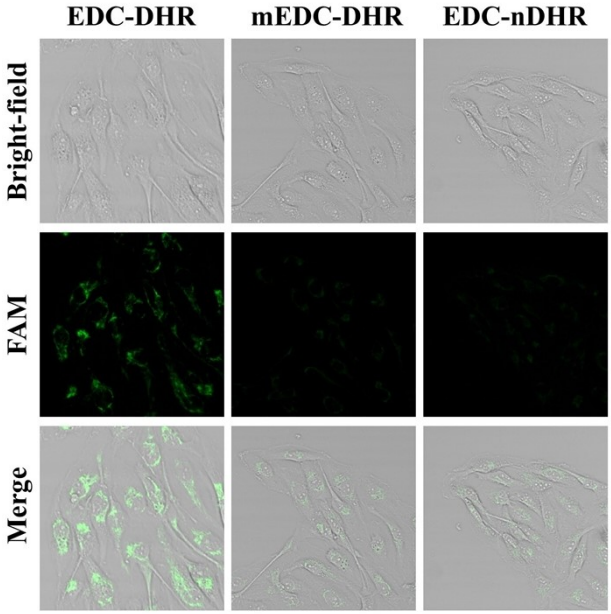

Figure S15. Low-magnification full-field image corresponding to Fig. 2B. The magnified area is marked by a red square. Scale bar: 25 μm.

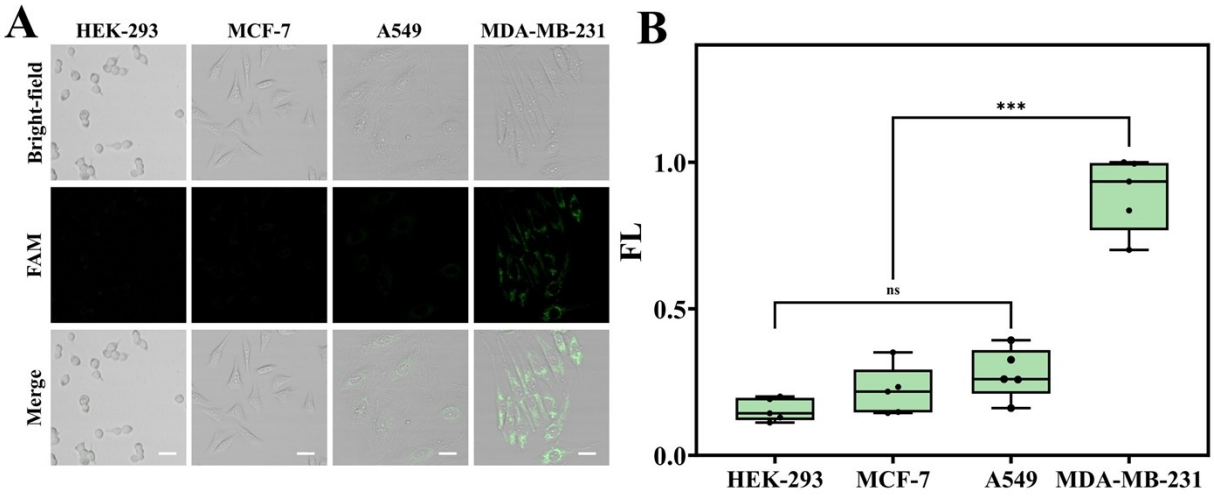

Figure S16. (A) Low-magnification full-field image corresponding to Fig. 3B. The magnified area is marked by a red square. Scale bar: 25 μm. (B) Quantification of FAM fluorescence intensity in Fig 3B, with data as mean ± SD (n=5, ***$p < 0.001$).

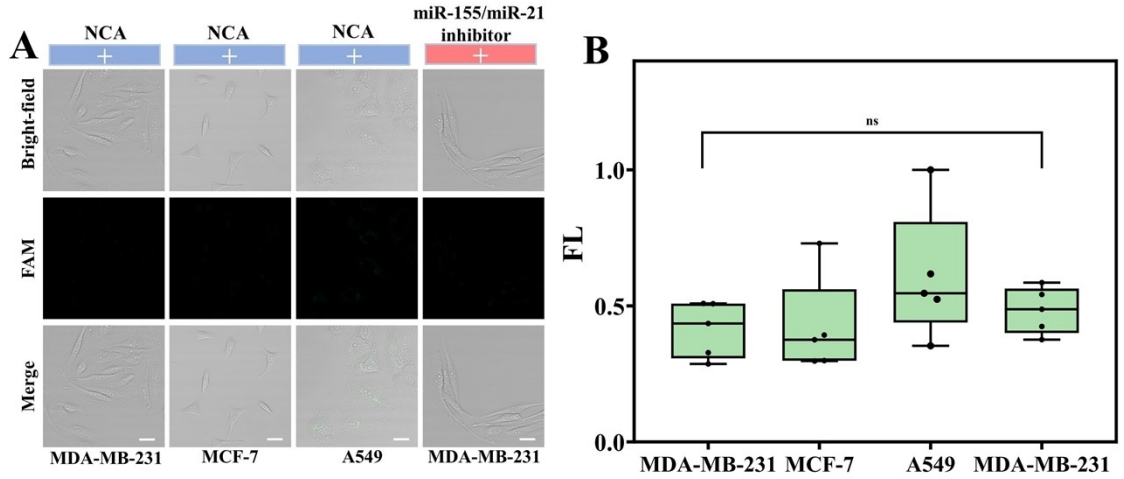

Figure S17. (A) Low-magnification full-field image corresponding to Fig. 3D. The magnified area is marked by a red square. Scale bar: 25 μm. (B) Quantification of FAM fluorescence intensity in Figure 3D. Data are presented as mean ± SD (n=5, ns: no significant difference).

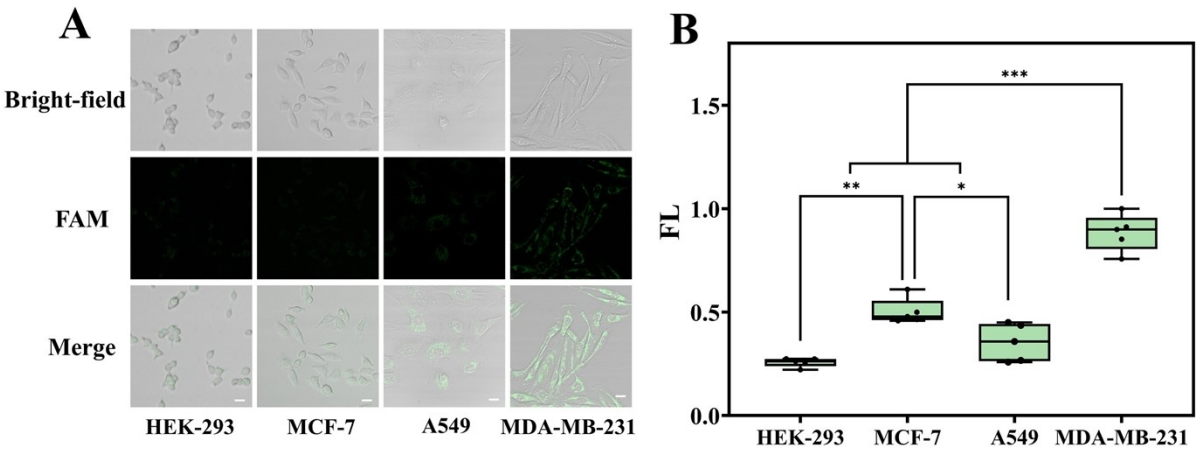

Figure S18. (A) CLSM images of the AND logic gate system in four cell lines: HEK-293, A549, MCF-7, and MDA-MB-231. All cells were incubated with the AND logic probe under identical conditions. Scale bar: 25 μm. (B) Quantification of FAM fluorescence intensity in (A), with data as mean ± SD (n=5, *$p < 0.05$, **$p < 0.01$, ***$p < 0.001$).

Quantitative fluorescence box plots verify that certain background signals occur in HEK-293, MCF-7 and A549 cells, apart from the target MDA-MB-231 cells. Nevertheless, HEK-293 cells still display the lowest background signal among all tested cell lines, and MDA-MB-231 cells maintain significantly superior fluorescence intensity with statistical differences.

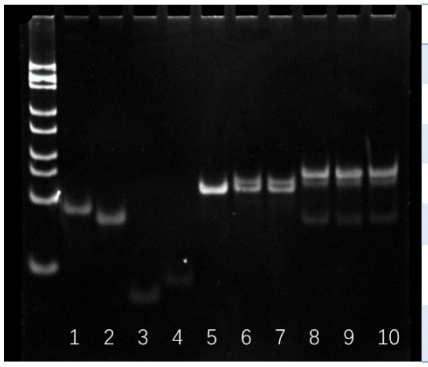

	1	2	3	4	5	6	7	8	9	10
S1	+				+	+	+	+	+	+
D1			+		+	+	+	+	+	+
D2				+	+	+	+	+	+	+
S2		+						+	+	+
APE1						+	+	+	+	+
miRNA21						+		+		+
miRNA155							+		+	+

Figure S19. Feasibility Analysis of the PAGE for the YES-OR Logic Detection System.

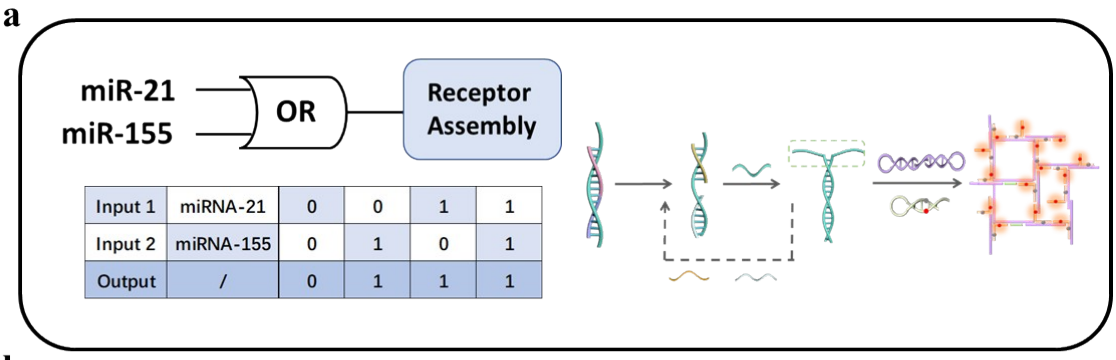

Figure S20. (a) Detection Principle and (b) PAGE Feasibility Analysis of the OR Logic Detection System.

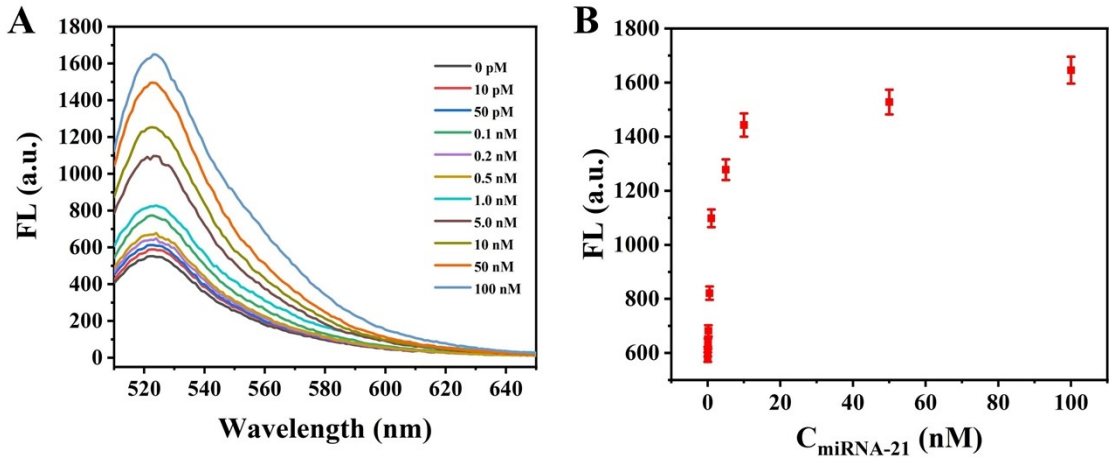

Figure S21. (A) Fluorescence intensity response curves of different concentrations of miRNA-21 upon addition of an identical amount of APE1 (10 U/ml); (B) Fluorescence detection plots for different concentrations of miR-21 in the presence of APE1 (10 U/mL) and miR-155 (100 nM). Data are presented as mean ± SD (n=3)

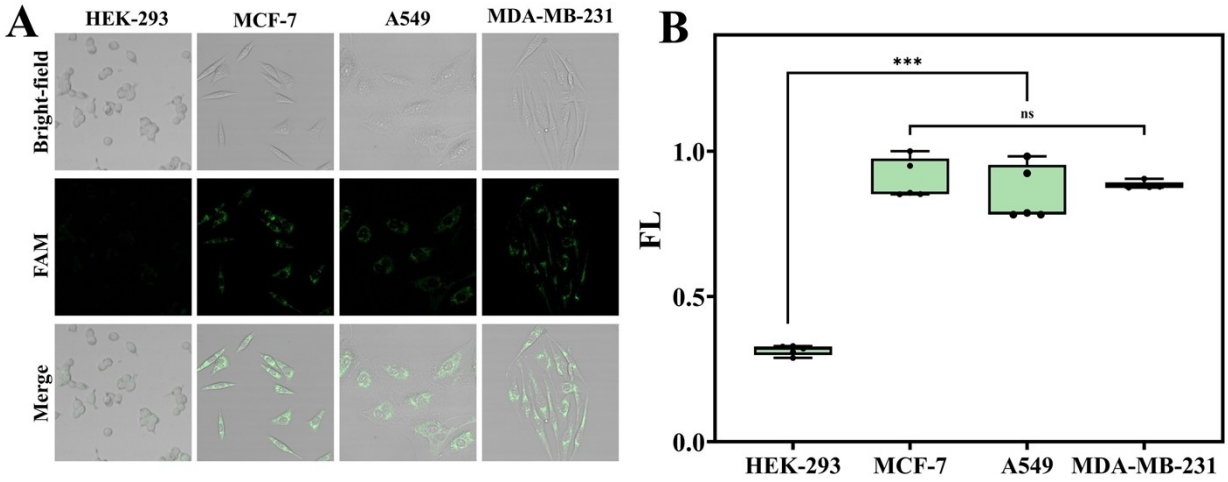

Figure S22. (A) Low-magnification full-field image corresponding to Fig. 4E. The magnified area is marked by a red square. Scale bar: 25 μm. (B) Quantification of FAM fluorescence intensity in Fig 4E, with data as mean ± SD (n=5, ***p < 0.001).

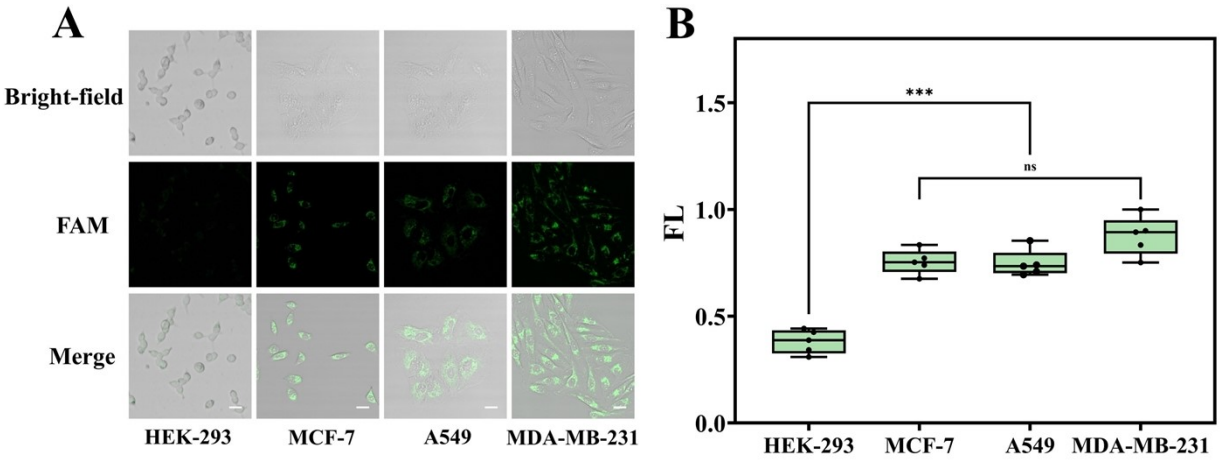

Figure S23. (A) Confocal laser scanning microscopy images demonstrating the feasibility of OR logic gates in different cell types. Scale bar: 25μm. (B) Quantification of FAM fluorescence intensity in (A), with data as mean ± SD (n=5, ***p < 0.001).

Quantitative fluorescence analysis reveals that weak yet detectable fluorescence signals exist in HEK-293 cells. In contrast, MCF-7, A549 and MDA-MB-231 cells all exhibit markedly enhanced fluorescent responses. Among all tested cell lines, MDA-MB-231 cells possess the highest fluorescence intensity.

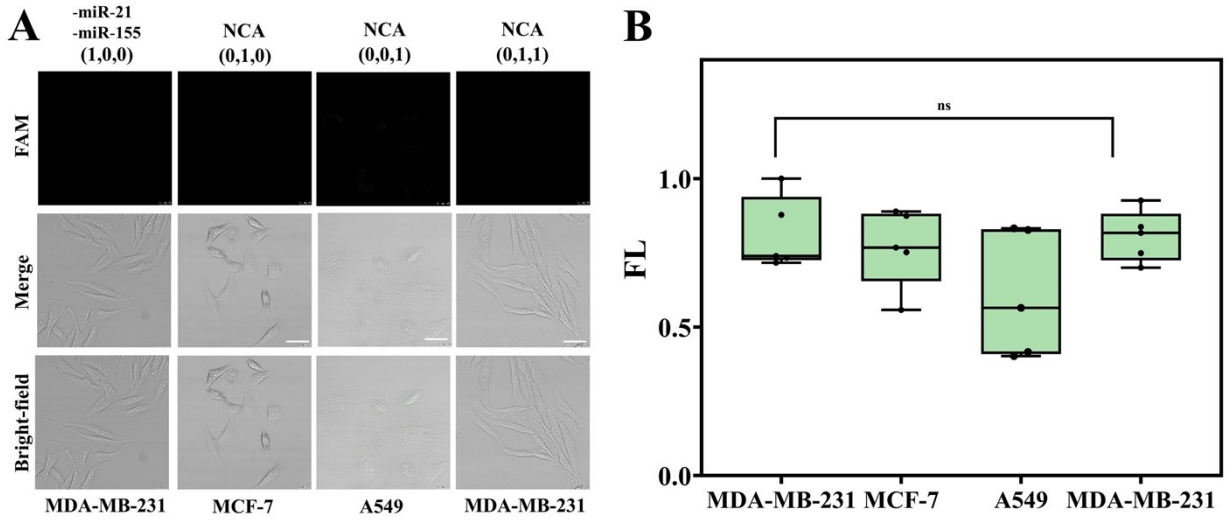

Figure S24. (A)Confocal laser scanning microscopy images of YES-OR logic gates regulating different cellular states. Scale bar: 25μm. (B) Quantification of FAM fluorescence intensity in (A). Data are presented as mean ± SD (n=5, ns: no significant difference).

Table S1. The DNA sequences used in this work.

Name	Sequences (5'-3')
S1	ACCCCTATCACGATTAGCATTAAACACCTGGGATCAAC ATCAGTCTGATAAGCTACCAG
YES-AND-S1	TAGCTTA/idSp/CAGACTGATGTTGATCCCAGGTGTTTAA TGCTAATCGTG/idSp/TAGGGGT
YES-OR-D1	TAGCTTA/idSp/CAGACTGATGTTGATCCCA
YES-OR-D2	GGTGTTTAATGCTAATCGTG/idSp/TAGGGGT
S2	CTAGAGCACATACAGACTGATGTTGATCCCAGGTGTTT AATGCTAATCGTG
AND-D1	CAGACTGATGTTGATCCCAGGTGTTTAATGCTAATCGT G
OR-D1	CAGACTGATGTTGATCCCA
OR-D2	GGTGTTTAATGCTAATCGTG
H1-1	GGTCTGATCCCTGGTAGCTTATTATGTGCTCTAGACAG TACTTTCGCTAGAGCACATAATAAGC
H1-2	GGATCAGACCCTGGTAGCTTATTATGTGCTCTAGACAG TACTTTCGCTAGAGCACATAATAAGC
H2	CTAGAG/FAM/CACATAATAAGCTACCAGTTTTTTGCTT ATTATGTG/BHQ1/CTCTAGCGAAAGTACTGT
miR-21	UAGCUUAUCAGACUGAUGUUGA
miR-155	UUAAUGCUAAUCGUGAUAGGGGU
miR-122	UGGAGUGUGACAAUGGUGUUUG
miR-141	UAACACUGUCUGGUAAAGAUGG
miR-144	UACAGUAUAGAUGAUGUACU
mismatched miRNA-21	UAACUUAUCAGACUGAUGUUGA
mismatched miRNA-155	UUAAUUCUAAUCGUGAUAGGGGU

Reference

(1) Garg, M.; Jain, N. K. Reduced hematopoietic toxicity, enhanced cellular uptake and altered pharmacokinetics of azidothymidine loaded galactosylated liposomes. *J Drug Target.* **2006**, *14* (1), 1-11.

(2) Maja, L.; Željko, K.; Mateja, P. Sustainable technologies for liposome preparation. *J Supercrit Fluid.* **2020**, *165*, 104984.